Hybrid passive/active inertial actuators to attenuate the structural response of a submerged hull

Peter J. Gangemi, Mauro Caresta and Nicole J. Kessissoglou

School of Mechanical and Manufacturing Engineering, The University of New South Wales, Sydney, Australia

ABSTRACT

This paper theoretically investigates the application of tuned vibration absorbers and hybrid passive/active inertial actuators to reduce the vibrational responses of plates and shells. The passive/active actuators are initially applied to a simple plate. A model of a submerged hull consisting of a ring stiffened finite cylinder with bulkheads and external fluid loading is then considered. The fluctuating forces from the propeller result in excitation of the low frequency global hull modes. Inertial actuators and tuned vibration absorbers are located at each end of the hull and in circumferential arrays to reduce the hull structural response at its axial resonances. The control performance of the hybrid passive/active inertial actuator, where the passive component is tuned to a structural resonance, is compared to the attenuation achieved by a fully passive tuned vibration absorber. This work shows the potential of using hybrid passive/active inertial actuators to attenuate the global structural responses of a submerged vessel.

INTRODUCTION

Since the theory was invented by Frahm (1911), tuned vibration absorbers (TVAs) have been successfully used to reduce the vibration and structure-borne sound of a variety of structures such as beams (Brennan & Dayou 2000; El-Khatib, Mace & Brennan 2005) plates (Snowdon 1975; Nicholson & Bergman 1986; Jolly & Sun 1996) and cylindrical shells (Huang & Fuller 1998). Advantages of the TVA include being relatively simple to implement, not requiring external energy to operate and never driving the system to instability. Jolly and Sun (1996) applied a TVA to a plate to attenuate the modes which strongly couple with the acoustic environment. Huang and Fuller (1998) examined the application of vibration absorbers to a cylindrical shell to attenuate the structural response and interior acoustic pressure.

Inertial actuators consist of a mass supported by a spring and driven by an external force, where typically the mass is much less than that of an absorber. A model of an inertial actuator which can be installed directly on the structure is described by Benassi, Elliott & Gardonio (2004). The transmitted force, blocked response and mechanical impedance for the inertial actuator are established. Benassi & Elliott (2005) showed that local application of an inertial actuator to a plate could reduce the plate global vibration response. It was found that the inertial actuator can provide large reductions in power, particularly when combined with outer velocity feedback control.

This paper presents a theoretical study investigating the use of tuned vibration absorbers and inertial actuators tuned to attenuate the vibrational response at structural resonances. The inertial actuators are initially applied to a plate with simply supported and free boundary conditions to attenuate the first three resonances. The actuators are then applied to a simplified physical model of a submarine hull. The performance of a hybrid passive/active inertial actuator is compared to the attenuation achieved by a tuned vibration absorber.

INERTIAL ACTUATORS

Unlike reactive actuators, inertial actuators do not need to react off a base and thus can be installed directly onto a vibrating surface (Benassi, Elliott & Gardonio 2004). The inertial actuators consist of a mass M_a, a spring of stiffness K_a and a damper C_a. The electromagnetically generated force F_a acts between the mass and a receiver plate, as shown in Fig. 1. F_T, x_a and w_p respectively represent the transmitted force, mass displacement and plate displacement.

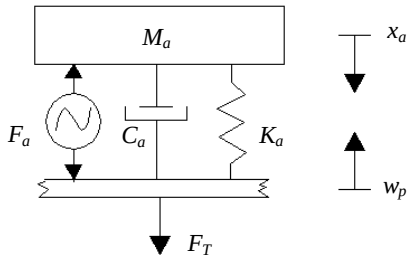

Figure 1. Dynamic model of the inertial actuator acting on a plate

The dynamic equation of the inertial actuator is given by (Benassi, Elliott & Gardonio 2004)

$$M_a\ddot{x}_a + C_a(\dot{x}_a + \dot{w}_p) + K_a(x_a + w_p) = -F_a \quad (1)$$

The transmitted force of the inertial actuator, F_T, to the plate is then described by

$$F_T = Z_a\dot{w}_p + T_aF_a \quad (2)$$

where the blocked response of the actuator, T_a, and the mechanical impedance, Z_a, are respectively given by

$$T_a = \frac{-\omega^2 M_a}{K_a - \omega^2 M_a + j\omega C_a} \tag{3}$$

$$Z_a = \frac{j\omega M_a K_a - \omega^2 M_a C_a}{K_a - \omega^2 M_a + j\omega C_a} \tag{4}$$

ω represents the radian frequency and j is the imaginary unit. Setting the control force, F_a, to zero simplifies the inertial actuator to the case of a tuned vibration absorber.

PASSIVE/ACTIVE CONTROL OF A PLATE

Figure 2 shows a rectangular plate with an external primary point force, F_p, and an inertial actuator. The plate has parallel simply supported boundary conditions at $y = 0$ and $y = L_y$ and free edges at $x = 0$ and $x = L_x$. The point force is located at (x_p,y_p) and the inertial actuator is located at (x_a,y_a).

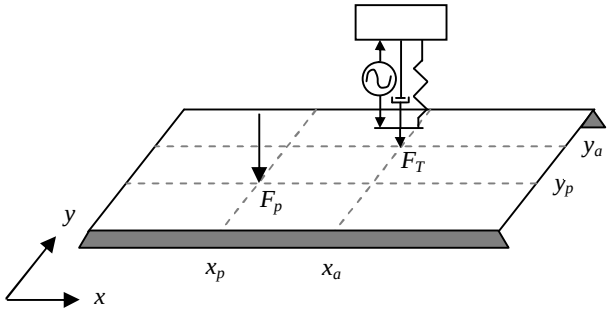

Figure 2. Locations of the primary force and inertial actuator for a rectangular plate

Due to the boundary conditions, the flexural displacement of the plate is composed of a modal solution in the y-direction and a wave solution utilised for the eigenfunction in the x-direction. For a plate with a single point force and single inertial actuator, the flexural displacement of the plate can be described by

$$w_{p1}(x,y,t) = \sum_{m=1}^{\infty} (A_1 e^{-jk_x x} + A_2 e^{jk_x x} + A_3 e^{-k_n x} + A_4 e^{k_n x}) \sin(k_y y) e^{j\omega t} \quad 0 \le x \le x_p \tag{5}$$

$$w_{p2}(x,y,t) = \sum_{m=1}^{\infty} (B_1 e^{-jk_x x} + B_2 e^{jk_x x} + B_3 e^{-k_n x} + B_4 e^{k_n x}) \sin(k_y y) e^{j\omega t} \quad x_p \le x \le x_a \tag{6}$$

$$w_{p3}(x,y,t) = \sum_{m=1}^{\infty} (C_1 e^{-jk_x x} + C_2 e^{jk_x x} + C_3 e^{-k_n x} + C_4 e^{k_n x}) \sin(k_y y) e^{j\omega t} \quad x_a \le x \le L_x \tag{7}$$

where L_x is the length of the plate. k_x and k_n are the modal wavenumbers for the propagating and evanescent waves in the x-direction, respectively. $k_y = m\pi/L_y$ is the modal wavenumber in the y-direction, where m is the mode number. The twelve unknown coefficients A_j, B_j and C_j for $j = 1$ to 4 are obtained from the continuity equations at the primary force location, the continuity equations at the inertial actuator and the boundary conditions of the plate. The continuity equations at the primary force and the actuator relate to the continuity of displacement, slope, bending moment and shear force. The boundary conditions at the free edges $x = 0$ and $x = L_x$ are zero bending moment and zero shear force. The unknown coefficients A_j, B_j and C_j may be solved by

$$\mathbf{A} = \boldsymbol{\alpha}^{-1}\mathbf{F} \tag{8}$$

where $\boldsymbol{\alpha}$ is a 12 × 12 matrix in terms of the continuity and boundary equations. The coefficient matrix $\mathbf{A}$ and the force matrix $\mathbf{F}$ are respectively given by

$$\mathbf{A} = \begin{bmatrix} A_1 & A_2 & A_3 & A_4 & B_1 & B_2 & B_3 & B_4 & C_1 & C_2 & C_3 & C_4 \end{bmatrix}^T \tag{9}$$

$$\mathbf{F} = \begin{bmatrix} 0 & 0 & 0 & 0 & 0 & 0 & 0 & \frac{2F_p}{L_y D}\sin(k_y y_p) & 0 & 0 & 0 & \frac{2F_a}{L_y D} T_a \sin(k_y y_a) \end{bmatrix}^T \tag{10}$$

D is the flexural rigidity of the plate. The non zero terms in $\mathbf{F}$ coincide with the rows in $\boldsymbol{\alpha}$ corresponding to the shear force at $x = x_p$ and $x = x_a$.

PASSIVE/ACTIVE CONTROL OF A SUBMERGED HULL

Dynamic response of a cylindrical shell

The submerged hull is modelled as a ring-stiffened finite cylindrical shell separated into compartments by internal bulkheads and submerged in fluid. At low frequencies where the fluid wavelength is large compared to the dimensions of the hull, the ends of the cylinder behave as monopoles and can be simplified as rigid end plates. Lumped masses are located at each end plate to represent the ballast tanks and allow for neutral buoyancy of the vessel to be achieved. A distributed mass on the shell accounted for onboard machinery such as the engines, generators and auxiliary equipment. An axial excitation force is applied at $x = 0$ to simulate excitation due to the transmission of fluctuating forces from the propeller through the shafting system. A schematic diagram of the submerged hull is given in Fig. 3.

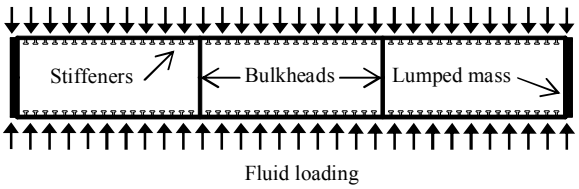

Figure 3. Schematic diagram of the submarine hull

For a cylindrical shell, the axial u_c, circumferential v_c, and radial w_c motions are the orthogonal components of the cylinder displacement in the x, θ and z directions, respectively, as shown in Fig. 4. a is the mean radius of the shell, h_c is the shell thickness and L is the length of the cylinder.

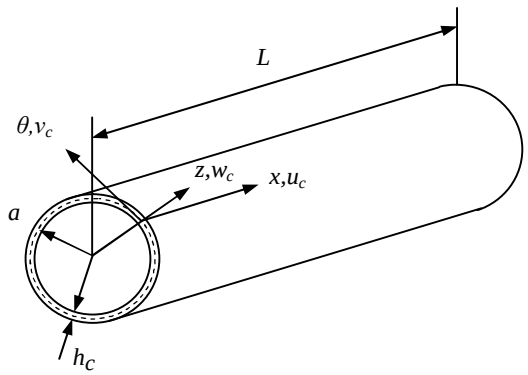

Figure 4. Displacements and coordinate system for a thin walled cylindrical shell.

The cylindrical shell is modelled using the Donnell-Mushtari equations of motion. The effects of the ring stiffeners are smeared across the surface of the hull, resulting in the structure being treated as an unstiffened cylinder with orthotropic properties. The smeared approach is accurate for low frequencies where the structural wavelength is much larger than the stiffener spacing (Hoppmann 1958). The stiffeners and onboard machinery are accounted for using additional terms in the Donnell-Mushtari equations. Fluid loading on the hull is modelled in terms of an acoustic impedance. The excitation of the hull from the propeller-shafting system is modelled as an axial force at one end of the stiffened cylinder. This gives rise to an axisymmetric response, allowing the equations of motion for the axial and radial motions to become uncoupled from the equation of motion for circumferential motion. The equations of motion for the stiffened cylindrical shell are then given by (Merz et al. 2007)

$$\frac{\partial^2 u_c}{\partial x^2} + \frac{\upsilon_c}{a}\frac{\partial w_c}{\partial x} - \left(1 + \frac{A_r}{bh_c} + \frac{m_d}{\rho_c h_c}\right)\frac{1}{c_L^2}\frac{\partial^2 u_c}{\partial t^2} = 0 \qquad (11)$$

$$\frac{\upsilon_c}{a}\frac{\partial u_c}{\partial x} + \left(1 + \frac{E_r A(1-\upsilon_c^2)}{E_c b h_c}\right)\frac{w_c}{a^2} + \beta^2\left(a^2\frac{\partial^4 w_c}{\partial x^4}\right) + \left(1 + \frac{A_r}{bh_c} + \frac{m_f}{\rho_c h_c}\right)\frac{1}{c_L^2}\frac{\partial^2 w_c}{\partial t^2} + \frac{r_f}{\rho_c h_c}\frac{1}{c_L^2}\frac{\partial w_c}{\partial t} = 0 \qquad (12)$$

where υ_c, ρ_c and E_c are respectively the Poisson's ratio, density and Young's Modulus of the hull. A_r and E_r correspond to the cross sectional area and Young's Modulus of the stiffeners, and b is the stiffener spacing. m_d represents the additional mass density to account for onboard equipment. $c_L = \sqrt{E_c/\rho_c(1-\upsilon_c^2)}$ is the longitudinal wavespeed of the hull. $\beta = h_c/\sqrt{12}\,a$ is a non-dimensional thickness parameter and m_f, r_f are respectively the fluid reactance and resistance (Junger & Feit 1986).

Substituting the general solutions into the stiffened cylindrical shell equations (11) and (12) results in a third order dispersion equation in terms of the squared structural wavenumber k_s^2. In the absence of torsional motion, the three axial wavenumbers for wave motion in the positive and negative directions correspond to a propagating wave and two standing waves. Omitting the harmonic term $e^{-j\omega t}$, the complete solutions of the displacements of the cylindrical shell can be written as

$$u_c(x) = \sum_{i=1}^{6} C_i W_i e^{jk_{s,i}x}, \quad w_c(x) = \sum_{i=1}^{6} W_i e^{jk_{s,i}x} \qquad (13, 14)$$

where in the absence of torsional motion, i = 1 to 6 represents the number of waves. U and W are respectively the wave amplitudes in the axial and radial directions. The ratio of the axial to radial displacement amplitudes is given by $C = \frac{U}{W}$.

Dynamic Response of the Bulkheads

The internal bulkheads are modelled as finite circular plates. The equations of motion for the out-of-plane w_b and in-plane u_b displacements of the circular plates are given by (Tso & Hansen 1995)

$$\nabla^4 w_b - (\rho_b \omega^2 h_b / D_b) w_b = 0 \qquad (15)$$

$$\frac{\partial}{\partial r}\left(\frac{\partial u_b}{\partial r} + \frac{1}{r}u_b\right) + \frac{\omega^2 \rho_b (1-\upsilon_b)}{E_b} u_b = 0 \qquad (16)$$

$\nabla^4 = \nabla^2\nabla^2$ where $\nabla^2 = \frac{\partial^2}{\partial r^2} + \frac{1}{r}\frac{\partial}{\partial r}$ is the Laplacian operator for axisymmetric motion. D_b, ρ_b, h_b, E_b and υ_b are the plate flexural rigidity, bulkhead density, thickness, Young's modulus and Poisson's ratio, respectively. r is the radial coordinate from the plate centre. General solutions to the equations of motion of a circular plate are given by (Tso & Hansen 1995)

$$w_b = A_{b1} J_0(k_{pB} r) e^{-j\omega t} + A_{b2} I_0(k_{pB} r) e^{-j\omega t} \qquad (17)$$

$$u_b = B_{b1} k_{pL} J_1(k_{pL} r) e^{-j\omega t} \qquad (18)$$

where I_0 is the modified Bessel function of the first kind of order zero. k_{pB} and k_{pL} are the bending and in-plane structural wavenumbers. The coefficients A_{b1}, A_{b2} and B_{b1} are determined from the boundary conditions for the submerged hull.

Boundary Conditions

The hull is divided into sections by the internal bulkheads and by the arrays of inertial actuators around the circumference of the hull. Inertial actuators are also located in an axial direction at each end of the hull. At each bulkhead/cylinder junction and each inertial actuator array/cylinder junction, continuity of displacement and slope as well as equilibrium of forces and moments is required. The notation of the forces, moments and displacements is shown in Fig. 5. F_{cx}, F_{cr} and M_c are the longitudinal force, transverse force and bending moment of the cylinder per unit length of the circumference. F_{bx}, F_{br} and M_b are the transverse force, radial force and bending moment of the circular plate per unit length of the outer radius.

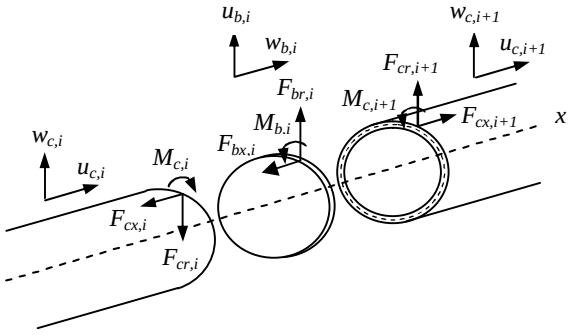

Figure 5. Notation and positive direction for all displacements, forces and moments of the hull and bulkheads.

The cylinder is supported at each end by rigid end plates which require three boundary conditions relating to the displacement, slope and force equilibrium. Nine continuity equations are required at each bulkhead/cylinder junction (Dylejko 2008). For a submerged hull consisting of two internal bulkheads, rigid end plates and a single array of actuators around the hull circumference, the unknown coefficients $\mathbf{A_c}$ correspond to the wave amplitudes of the cylinder segments and internal circular plates. The unknown coefficients can be obtained from the matrix $\boldsymbol{\alpha}_\mathbf{c}\,\mathbf{A_c} = \mathbf{F_c}$ expression, where

$\boldsymbol{\alpha}_c$ is a matrix from the assembly of the boundary and continuity equations and $\mathbf{F}_c$ is a force vector.

For the array of inertial actuators located circumferentially around the hull, the passive component of the actuator force corresponding to $F_T = Z_a \dot{w}_c$ is included in the expression for force equilibrium in the radial direction.

$$F_{cr,i} - F_{cr,i+1} + F_T = 0 \tag{19}$$

When an inertial actuator is applied axially, the passive element of the actuator force corresponding to $F_T = Z_a \dot{u}_c$ is added into the boundary conditions for the rigid end plates at $x = 0$ and $x = L$ and the expressions become

$$m_l \frac{\partial^2 u_c}{\partial t^2} = F_p - 2\pi a F_{cx} + F_T, \qquad x = 0 \tag{20}$$

$$m_l \frac{\partial^2 u_c}{\partial t^2} = 2\pi a F_{cx} + F_T, \qquad x = L \tag{21}$$

where F_p is the axial excitation force applied to the hull end plate at $x = 0$. The axial force simulates excitation due to the transmission of fluctuating forces from the propeller through the shafting system. m_l represents the lumped masses at each end.

The active element of the inertial actuators is modelled through the force matrix $\mathbf{F}_c$. The only non zero terms in the force matrix correspond to the active component of the inertial actuator $\frac{T_a F_a}{2\pi a}$, for an actuator located at $x = 0$, at $x = L$ and an array of actuators around the circumference.

RESULTS

Structural response of the plate

Results are initially presented for the plate with length L_x = 1.4m, width L_y = 0.5m and thickness h = 0.002m. The material used for the plate is steel with a density ρ = 7800kgm^{-3}, Young's modulus $E = 2.1\times10^{11}$Nm^{-2} and Poisson's ratio υ = 0.3. Structural damping was introduced using a complex Young modulus $E(1 - j\eta)$, where η = 0.02 is the structural loss factor. The inertial actuators applied to the plate have a mass of M_a = 0.1kg, damping ratio ζ = 0.03 and the required stiffness value K_a and damping constant C_a to tune the device to the desired resonance. The point force excitation F_p has a unity magnitude and is applied on the plate at an arbitrary location of (x_p, y_p) = (0.6m, 0.2m). The inertial actuators for the first, second and third targeted resonances respectively are located along the same x-coordinate as F_p at (x_a, y_a) = (0.6m, 0.3m), (x_a, y_a) = (0.6m, 0.35m) and (x_a, y_a) = (0.6m, 0.4m).

The low frequency resonances associated with flexural vibration of the steel plate are examined. The frequency response function for the primary response at an arbitrary error sensor location of (x_e, y_e) = (0.4m, 0.4m) is shown in Figs. 6 to 10. At low frequencies, the first three dominant peaks have a frequency of 19.5Hz, 29Hz and 39.5Hz. A single inertial actuator is applied to the plate and the passive component is tuned in close proximity to the frequency of the particular resonance to be attenuated. The natural frequency of the passive component is selected as to maximise the attenuation achieved at each structural resonance. Initially, only the passive element is utilised for control and the results are shown in Figs 6 to 9. In Fig. 6, the passive element of the actuator is tuned to 19.5Hz, close to the first resonant frequency, achieving attenuation of 20dB at this frequency. In Fig. 7, the passive element of the inertial actuator is tuned to 29Hz, resulting in a 20dB reduction at the second dominant peak. In Fig 8, the passive element of the actuator is tuned to 39.5Hz, achieving a 15dB reduction in the structural response at the third targeted frequency. Figure 9 presents the results using three inertial actuators with passive elements tuned to the three targeted resonant frequencies respectively. Attenuation levels achieved at the three dominant peaks using the three actuators simultaneously match the reductions in structural vibration obtained by using a single actuator at a time. In Fig. 10, the effect of the hybrid passive/active inertial actuator is shown. At the first resonance, 30dB in attenuation is achieved, compared to 20dB using only the passive device. The amplitude of the required control force at the first resonance is $F_a = 0 + 0.0971i$, which is significantly lower than the unity magnitude of the primary excitation.

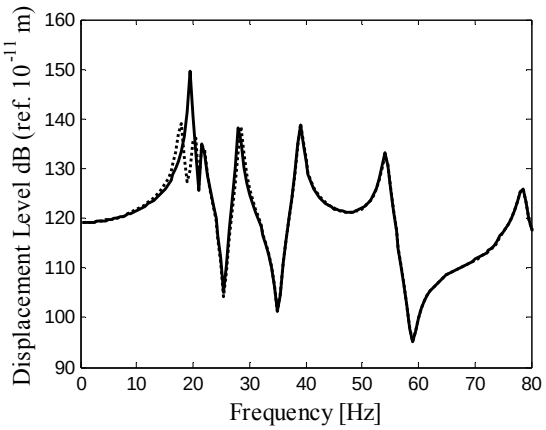

Figure 6. Frequency response function for the primary response of the plate (——), with the passive component of an inertial actuator tuned to 19.5Hz (· · ·) (passive control only).

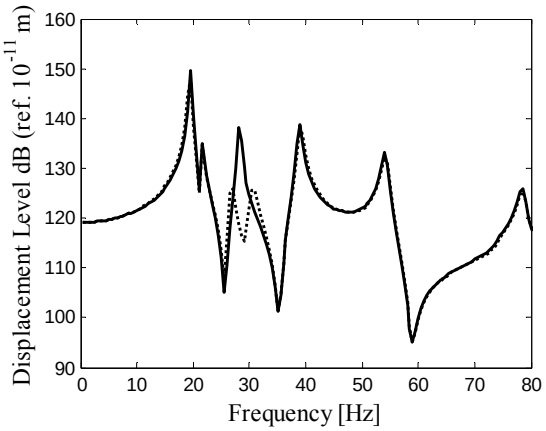

Figure 7. Frequency response function for the primary response of the plate (——), with the passive component of an inertial actuator tuned to 29Hz (· · ·) (passive control only).

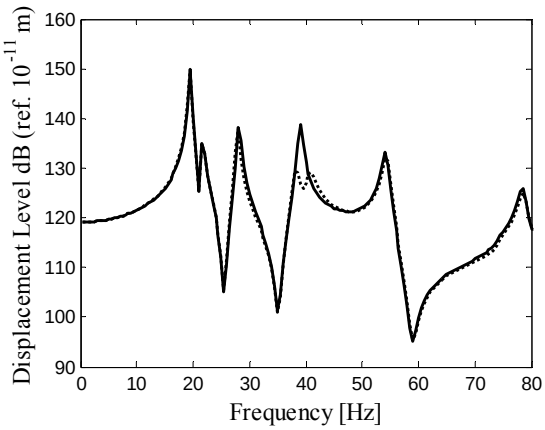

Figure 8. Frequency response function for the primary response of the plate (——), with the passive component of an inertial actuator tuned to 39.5Hz (· · ·) (passive control only).

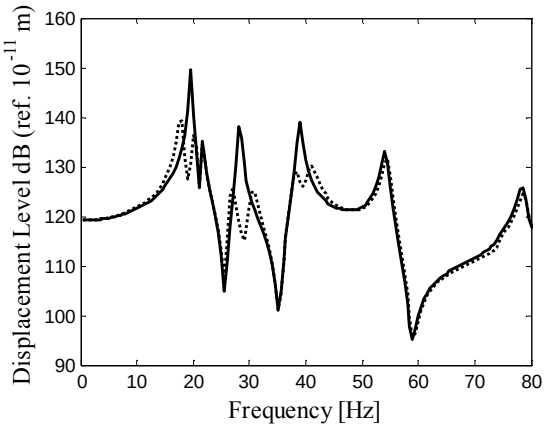

Figure 9. Frequency response function for the primary response of the plate (——), with the passive components of three inertial actuators respectively tuned to 19.5Hz, 29Hz and 39.5Hz (· · ·) (passive control only).

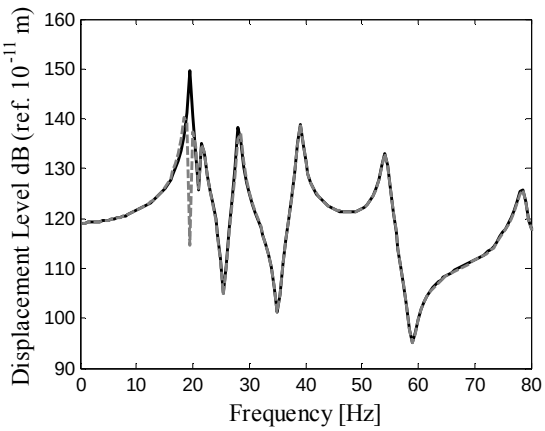

Figure 10. Frequency response function for the primary response of the plate (——), using a hybrid passive/active inertial actuator with the passive component tuned to 19.5Hz (– – –).

Submerged Hull

The ring-stiffened cylindrical hull has a radius a = 3.25m, hull thickness h_c = 0.04m, length L = 45m and with two evenly spaced bulkheads of thickness h_b = 0.04m. The material properties of the steel used for the hull, bulkheads and stiffeners are identical to those used for the plate. The internal stiffeners have a rectangular cross-section of A_r = 0.08m × 0.15m and are evenly spaced by a distance of b = 0.5m. The thickness of the circular plates at each end of the cylinder is the same as for the bulkheads (h_b = 0.04m). The onboard equipment and ballast tanks were taken into account by considering lumped masses at each end of the hull of m_l = 2×10^5 kg and a distributed mass on the shell surface of m_d = 1500kgm^{-2}. The inertial actuators at each end of the submerged hull have a total mass of $M_a = 10^4$kg, damping ratio ζ = 0.03 and a stiffness value of K_a and damping constant C_a appropriately selected for each individual resonance. The actuator array around the circumference of the hull consists of 200 actuators and has a total mass of $M_a = 6\times10^4$kg as well as a damping ratio of ζ = 0.03.

The low frequency response of the submerged hull with inertial actuators is investigated. The frequency response function of the uncontrolled hull axial displacement at x = 0 and $x = L$ is shown in Fig. 11. Rigid body motion occurs at the zeroth natural frequency due to the hull being a free-free system. The first three hull axial resonances occur at 21.8Hz, 44.8Hz and 69.7Hz. The resonant frequencies of the bulkheads can also be observed at 9.4Hz and 36.4Hz. In Fig. 12, the passive element of an inertial actuator is tuned to the first hull axial frequency at 21.8Hz and attached at the end plate at $x = L$. It can be seen that when only the passive component is utilised, significant attenuation is achieved at the targeted resonance. The response from the hybrid passive/active inertial actuator is similar to the passive element, except for the additional attenuation provided at the resonant frequency.

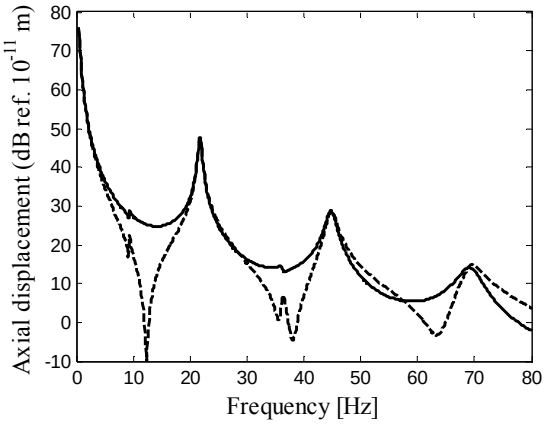

Figure 11. Frequency response function of the submerged hull at x=0 (– – –), at x=L (——).

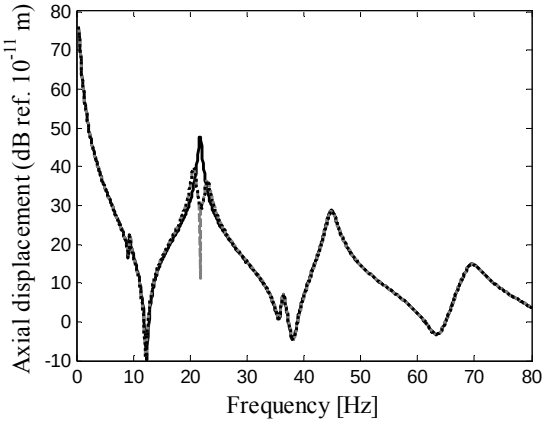

Figure 12. Frequency response function at x=0 (——), with the passive component of an inertial actuator at x=L (· · ·), with the application of a hybrid passive/active inertial actuator at x=L (– – –).

Figure 13 presents similar results to those in Fig. 12 but with the inertial actuator now located at x = 0, with the passive component also tuned to the first hull axial frequency of 21.8Hz. It is observed that slightly more attenuation is achieved from both the passive only and hybrid passive/active system when the inertial actuator is attached to the end plate at x = 0 compared to when it is attached at x = L. This is attributed to the matching of the modeshape function values at the primary source and secondary source locations. Figure 14 presents the uncontrolled and controlled results when an array of actuators tuned to 21.8Hz is located around the circumference of the hull at x = L/2. In this case, the actuators are acting in the radial direction, thereby having a negligible effect on the axial displacement.

The effect of the inertial actuators on the axial and radial acceleration levels along the length of the hull at the first hull axial resonance is investigated. The application of a single actuator located at x = L, an actuator located at x = 0 and an array of actuators located circumferentially around the hull at x = L/2, is respectively shown in Figs. 15 to 17. The impact of the bulkheads at 15m and 30m is clearly visible for the radial responses. In Figs. 15(a) and 15(b), attenuation of up to 15dB in the axial and radial acceleration levels is obtained using the passive element of the actuator. The hybrid passive/active actuator achieves further gains of up to 10dB in the axial and radial acceleration levels along the length of the hull. The attenuation achieved by the fully active/passive system is globally greater when the actuator is located at x = 0 compared to x = L. Fig. 17 shows that when an array of actuators is positioned around the circumference of the hull at x = L/2, the effect of both the passive component and the hybrid passive/active inertial actuators on the axial acceleration is minimal. The impact of the array on the radial acceleration levels is restricted to the location of the array at x = L/2 with the inertial actuator achieving attenuation of 20dB compared to 5dB for the passive system. Table 1 shows the control force magnitude of the inertial actuators at the first hull axial resonance. For all cases, the control force magnitude is significantly lower than the unity primary axial excitation.

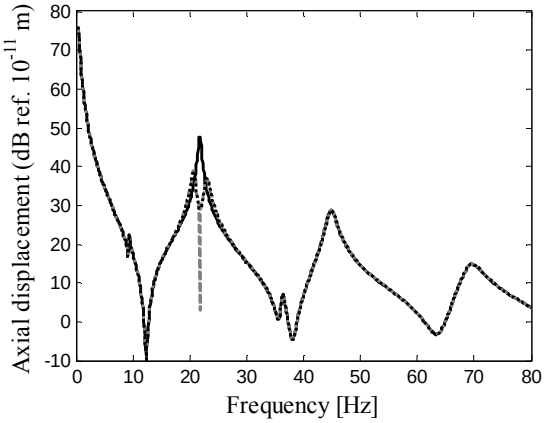

Figure 13. Frequency response function at x=0 (——), with the passive component of an inertial actuator at x=0 (· · ·), with the application of a hybrid passive/active inertial actuator at x=0 (– – –).

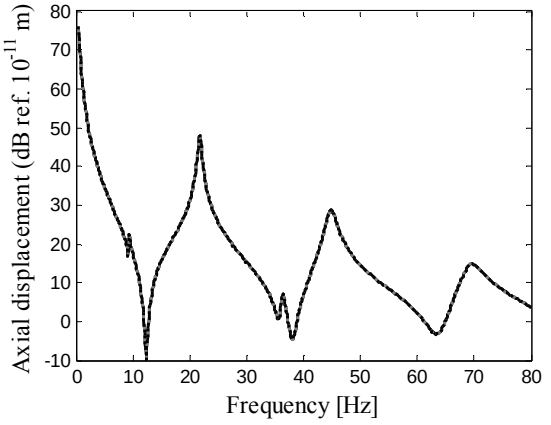

Figure 14. Frequency response function at x=0 (——), with the passive component of an array of inertial actuators at x=L/2 (· · ·), with the application of an array of hybrid passive/active inertial actuators at x=L/2 (– – –).

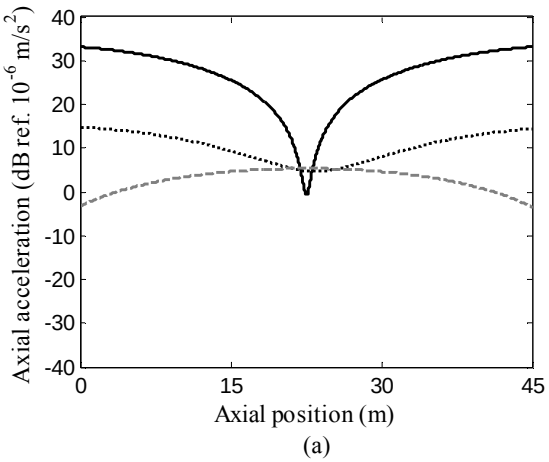

(a)

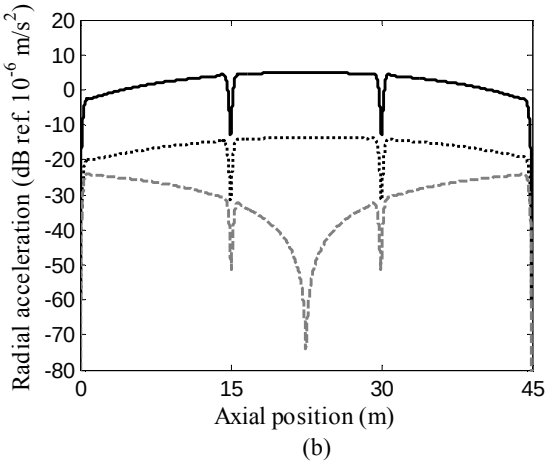

(b)

Figure 15. Axial (a) and radial (b) responses at the first axial resonance of 21.8Hz; uncontrolled response (——), with the passive component of an inertial actuator at x=L (· · ·), with the application of a hybrid passive/active inertial actuator at x=L (– – –).

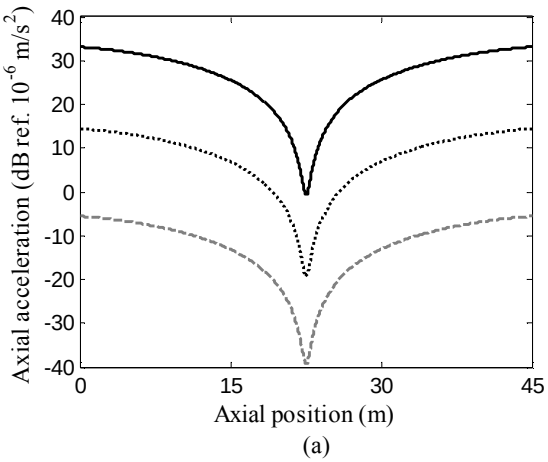

(a)

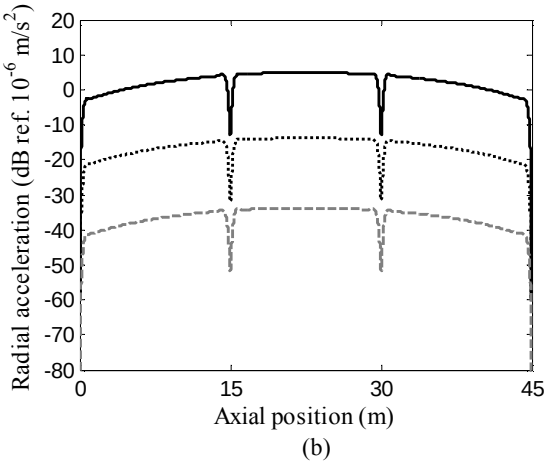

(b)

Figure 16. Axial (a) and radial (b) responses at the first axial resonance of 21.8Hz; uncontrolled response (——), with the passive component of an inertial actuator at x=0 (· · ·), with the application of a hybrid passive/active inertial actuator at x=0 (– – –).

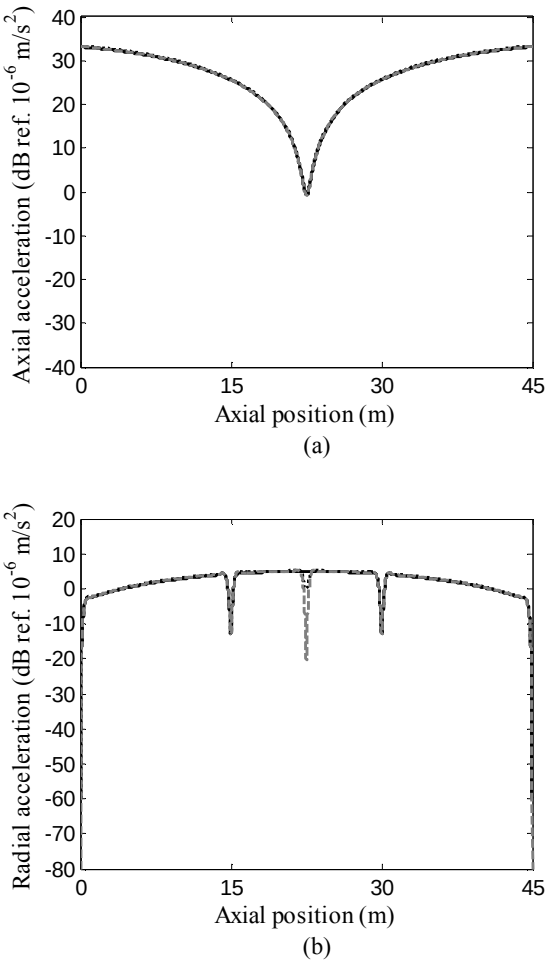

Figure 17. Axial (a) and radial (b) responses at the first axial resonance of 21.8Hz; uncontrolled response (——), with the passive component of an array of inertial actuators at $x=L/2$ (· · ·), with the application of an array of hybrid passive/active inertial actuators at $x=L/2$ (– – –).

Table 1. Control force magnitudes

Actuator location	F_a
$x = L$	$0 - 0.054i$
$x = 0$	$0.0007 + 0.00533i$
$x = L/2$	$-0.0374 - 0.0314i$

CONCLUSIONS

Attenuation of the vibrational response using hybrid passive/active methods has been presented for two structures. Inertial actuators were applied to a plate and to a simplified model of a submerged hull. The control performance using a passive control system and a hybrid passive/active system are compared. A reduction of up to 20dB in the plate response was achieved for the first three dominant resonances using the passive component of the inertial actuators, and up to 30dB attenuation was achieved using hybrid passive/active system. Inertial actuators were applied to a submerged hull and tuned to the first hull axial resonance. Attenuation of the axial and radial acceleration levels of up to 20dB was obtained using the passive component of the inertial actuators, and up to 30dB using the hybrid passive/active actuator. At the hull axial resonances, the control measures applied to the end plates at each end of the hull were more successful in reducing the structural response than the arrays located around the hull circumference. This work has shown that the use of hybrid passive/active inertial actuators have the potential to reduce the low frequency vibrational responses of a submerged hull.

ACKNOWLEDGEMENT

The authors would like to acknowledge the financial contribution from the New South Wales division of the Australian Acoustical Society to attend Acoustics 2011.

REFERENCES

Benassi, L and Elliott, SJ 2005, 'Global control of a vibrating plate using a feedback-controlled inertial actuator', *Journal of Sound and Vibration*, vol. 283, pp. 69-90.

Benassi, L, Elliott, SL & Gardonio, P 2004, 'Active vibration isolation using an inertial actuator with local force feedback control', *Journal of Sound and Vibration*, vol. 276, pp. 157-179.

Brennan, MJ & Dayou, J 2000, 'Global control of vibration using a tunable vibration neutralizer', *Journal of Sound and Vibration*, vol. 232, no. 2, pp. 585-600.

Dylejko, P, 2008, 'Optimum resonance changer for submerged vessel signature reduction', PhD thesis, The University of New South Wales, Sydney.

El-Khatib, HM, Mace, BR & Brennan, MJ 2005, 'Suppression of bending waves in a beam using a tuned vibration absorber', *Journal of Sound and Vibration*, vol. 288, pp. 1157-1175.

Frahm, H 1911, *Device for damping vibrations of bodies*, US Patent 989958.

Hoppmann, WH 1958, 'Some characteristics of the flexural vibrations of orthogonally stiffened shells', *Journal of the Acoustical Society of America*, vol. 30, pp. 77-82.

Huang, YM & Fuller, CR 1998, 'Vibration and noise control of the fuselage via dynamic absorbers', *Journal of Vibration and Acoustics*, vol. 120, no. 2, pp. 496-502.

Jolly, MR & Sun, JQ 1996, 'Passive tuned vibration absorbers for sound radiation reduction from vibrating panels', *Journal of Sound and Vibration*, vol. 191, no. 4, pp. 577-583.

Junger, MC & Feit, D 1986, *Sound, structures and their interaction*, Second edition, MIT Press, Cambridge.

Merz, S, Oberst, S, Dylejko, PG, Kessissoglou, NJ, Tso, YK & Marburg, S 2007, 'Development of coupled FE/BE models to investigate the structural and acoustic responses of a submerged vessel', *Journal of Computational Acoustics*, vol. 15, pp. 23-47.

Nicholson, JW & Bergman, LA 1986, 'Vibration of damped plate-oscillator systems', *Journal of Engineering Mechanics*, vol. 112, pp. 14-30.

Snowdon, JC 1975, 'Vibration of simply supported rectangular and square plates to which lumped masses and dynamic vibration absorbers are attached', *Journal of the Acoustical Society of America*, vol. 57, no. 3, pp. 646-654.

Tso, YK & Hansen, CH 1995, 'Wave propagation through cylinder/plate junctions', *Journal of Sound and Vibration*, vol. 186, pp. 447-461.